

**HIGH BIT DENSITY MILLIMETER WAVE CHIPLESS RFID SYSTEMS
AND METHODS THEREOF**

FIELD

- 5 [0001] This technology generally relates to radio frequency identification (RFID) systems and, in particular, to high bit density chipless millimeter wave RFID systems and methods thereof.

BACKGROUND

- [0002] RFID technology makes use of item tags that fall into one of three
10 major categories: (1) active systems that include a local power source as part of the RFID tag and include circuitry or an integrated circuit (IC), or silicon chip, for communicating and storing identification or other data that is typically read using an RFID reader; (2) passive systems where the power required for the tag IC and communications with that IC is supplied by the RFID reader; and (3) chipless systems
15 that use tags without ICs, or chips, where the tags are read wirelessly by a device that reads and decodes information represented by various chipless technology methods.

- [0003] One of the major requirements in any RFID system is to store as much information as possible on the RFID tag. As chipless RFID systems do not use a semiconductor or “chip” storage device on the tag, the data stored on the tag must be
20 encoded and stored through some other mechanism. An important objective of chipless RFID system design is to keep the manufacturing costs of the tags, which store the encoded information, as low as possible. One approach to reduce the cost of chipless tags is to use printing methods that typically lay down an electrically conductive, or metallic, pattern on the tag substrate material. The printed patterns are
25 used to encode information as stored data. The RFID reader wirelessly interacts with the tag and decodes the data as a “read.” Different methods may be utilized to represent or encode data in the printed patterns on the tag. The more data that is represented in a given area is defined as the bit density of the chipless tag.

[0004] Various methods have been used to represent information in printed patterns. In one example, information is represented or encoded on a tag using a tuned circuit implemented through lumped-element switched resonant circuits. The tags are read through a spectrum signature approach, measuring magnitude response as a function of frequency. Broadband interrogating pulses are used to cover the range of tuned frequencies of the resonant circuits. The constraint on the number of bits represented per unit area is controlled by the physical size of the tuned circuit, and the tuning sharpness, or Q, of the circuit. The higher the Q of the tuned circuit, the more frequency discrimination or spectral signature discrimination is possible, which increases the ability to represent or encode more bits within a given tag area. However, Q is determined by the electrical conductivity of the resonant circuit elements. Thus, the system requires using high conductivity materials to increase bit density, which increases costs of manufacturing the tags. Further, the bit density using lumped element tuned circuits to generate distinct spectral signatures is only on the order of several bits per square inch area.

[0005] Other methods have used synthetic aperture radar (SAR) imaging to read data encoded in chipless tags, which increases the potential bit density by enabling the spatial imaging domain as another variable. These methods have utilized up to 60 GHz SAR imaging techniques.

[0006] One method has used meander line tag elements to encode the tags for SAR imaging, with an estimated upper bit density of 12 bits per square inch. Another approach uses a plurality of antenna elements instead of lumped element resonant circuits or meandered strip lines. At the limit of 60 GHz frequency described, the practical size of the antenna elements is on the order of 1.5mm x 1.5mm. More importantly, the parametric variables of element phase measurement and element polarization measurement in the example implementation shows 4 states for each, yielding a 4x4 or a 16-state code ($\text{Log}_2(16) = 4$ bits/element). Given the small size of the antenna elements at a 60 GHz operating frequency, approximately twenty-five

elements fit into a square inch of tag area with appropriate element to element isolation, which yields an estimated upper bit density at 100 bits per square inch.

[0007] In each of the methods described, the tag bit density is less than passive or active RFID systems where up to thousands of bits are stored within a memory chip or ASIC located on the tag itself, or separately connected to an external circuit or sensor.

SUMMARY

[0008] The present technology advantageously provides a system including chipless RFID readers and tags that optimizes the ability to achieve high tag bit densities, while reducing chipless tag cost. The system provides an increase in the RFID system operating frequency, which reduces the physical tag element size. The system advantageously utilizes small physical size printable tag element antennas based on the $\frac{1}{2} \lambda$ microstrip patch, which allows for small physical spacing between tag elements antennas that is optimized for low inter-element coupling.

[0009] The system further employs advanced synthetic aperture radar (SAR) and inverse synthetic aperture radar (ISAR) reader technology using fully polarimetric radar, which enables high-resolution polarization discrimination and high-resolution phase discrimination. The tag antenna elements utilized can be optimized to control polarization by altering the E-field rotational geometric orientation. The phase response can also be altered by changing the length and/or geometry of the antenna element phase structures that set the time delay of the reradiation energy. The combination of the imaging techniques and the increase the number of decodable polarization states and phase states for a single tag antenna element increases the bit density that can be achieved for the chipless tags utilized. The system can advantageously be used with low-cost printable electrically conductive materials that maintain high reradiation efficiency and high radar cross section (RCS) values.

Finally, the use of frequency modulated continuous wave (FMCW) SAR with a wide sweep bandwidth advantageously provides high image resolution.

[0010] The system can be advantageously employed and provide the
aforementioned advantages in any usage requiring RFID tag or sensor operation,
5 including, but not limited to: inventory identification; asset management tracking and
shipping container location; vehicular access control (*e.g.* toll ways); moving vehicle
identification; healthcare identification and tracking of patients, drugs, equipment and
personnel identification, tracking and monitoring of personnel and equipment for
security purposes; identification of luggage and packages at airports; systems for
10 locating lost objects (*e.g.* keys, files, golf balls, clothing articles), although any other
uses can be contemplated.

BRIEF DESCRIPTION OF THE DRAWINGS

[0011] FIG. 1 is a block diagram of an exemplary high-bit chip density
millimeter wave chipless RFID system of the present technology including an
15 exemplary millimeter wave RFID reader device interrogating an exemplary chipless
RFID tag.

[0012] FIG. 2A is a circuit diagram of transmitters, receivers, and frequency
control for an exemplary millimeter wave RFID reader device of the present
technology.

20 [0013] FIG. 2B is a schematic view of the subcarrier down conversion, data
acquisition, and signal processing of the exemplary millimeter wave RFID reader
device of the present technology shown in FIG. 2A.

[0014] FIGS. 3A and 3B are a front view and a side view of the antenna of the
exemplary millimeter wave RFID reader device of the present technology.

25 [0015] FIGS. 4A and 4B are circuit diagrams for the exemplary radar receiver
(FIG. 4A) and an exemplary the radar transmitter (FIG. 4B) shown in FIG. 2A.

[0016] FIG. 5 is a perspective view of an exemplary microstrip patch antenna on a substrate that may be utilized in the exemplary chipless RFID tag shown in FIG. 1.

[0017] FIG. 6A is a schematic view of an exemplary RFID chipless tag using 5 60 GHz as the SAR radar frequency.

[0018] FIG. 6B is a schematic view of an exemplary RFID chipless tag using 120 GHz as the SAR radar frequency.

[0019] FIG. 6C is a schematic view of an exemplary RFID chipless tag using 240 GHz as the SAR radar frequency.

10 [0020] FIG. 7 shows exemplary polarization state orientations that may be utilized for the microstrip patch antenna elements located on the exemplary RFID chipless tag of the present technology.

[0021] FIG. 8 shows exemplary elements that may be utilized to determine the phase state for the microstrip patch antenna elements located on the exemplary RFID 15 chipless tag of the present technology.

[0022] FIG. 9 shows exemplary polarization and phase state combinations that may be utilized for the microstrip patch antenna elements located on the exemplary RFID chipless tag of the present technology.

[0023] FIG. 10 is a flowchart of an exemplary inverse synthetic aperture radar 20 (SAR) processing method of the present technology.

[0024] FIG. 11 illustrates a simulation of the radar cross section of a conductive sheet as a function of sheet electrical conductivity for various materials.

[0025] FIG. 12 is a graph of material conductivity versus RCS for various materials and an associated table of material conductivities.

[0026] FIG. 13 is a graph of parameters for sweep bandwidth (B_{SH}) and sweep time (T_S) for the exemplary RFID reader device of the present technology.

[0027] FIG. 14 is an exemplary of digital data from the exemplary RFID reader device.

5 [0028] FIG. 15 is an exemplary spectrum for a SAR imaging analysis.

[0029] FIG. 16 is an exemplary experimental setup for generating SAR images in accordance with the present technology.

[0030] FIG. 17 illustrates polarization data extracted in a SAR imaging process.

10 [0031] FIG. 18 illustrates phase data extracted in a SAR imaging process.

DETAILED DESCRIPTION

[0032] An example of a high bit density millimeter wave chipless RFID system is illustrated in FIGS. 1-9. In this particular example, the system includes a polarimetric RFID reader device and a chipless RFID tag, although the system may include other types and/or numbers of other systems, device, components, and/or other elements in other combinations, including additional reader devices and any number of chipless RFID tags, by way of example only. The present technology advantageously provides a millimeter wave chipless RFID system that allows for increased bit density of information that may be encoded on the chipless tags. The present technology further minimizes the costs associated with manufacturing the chipless tags.

15

20

[0033] Referring now more specifically to FIGS. 1, 2A, and 2B, the exemplary RFID reader device utilizes fully polarimetric synthetic aperture radar (SAR) with high resolution polarization and phase discrimination detection that resolves both polarization and phase states, as described in further detail below. The specific type of

25

SAR radar architecture is application dependent, and can be enabled by either moving the RFID reader device (SAR) or the chipless tag (ISAR) that is being interrogated, or by using a fixed RFID reader device with an antenna array.

[0034] The RFID reader device of examples of the present technology is used
5 to image and decode the chipless RFID tags and utilizes wideband, frequency modulation continuous wave (FMCW) radar. FMCW radar may be advantageously utilized for short distance applications such as RFID. Traditionally, SAR radar used in aircraft and satellites uses pulse radar, where the radio frequency propagation time delay between the radar platform and the target area is long enough so that the radar
10 has time to switch between the transmitting mode and receiving mode. Typical pulse radar distances are in excess of 1 km, which defines the round trip time for a transmitted radar pulse to be greater than 6 μ s. However, for RFID systems, where in many cases the distance, or radar range, is on the order of a few meters, pulse radar switching is difficult due to the very short round trip time from the radar to the target
15 and back. For example, at 1 meter range from the RFID reader device to the tag, the round trip delay for the radar signal is less than 7 ns. If pulse type radar were used, it would require the ability to switch between the transmitting mode and receiving mode in less than 7 ns, which results in a challenging and costly radar design. FMCW radar transmits and receives at the same time, which eliminates a switching time between
20 transmitting and receiving modes. Accordingly, examples of the present technology employs FMCW radar for the exemplary RFID reader device.

[0035] For practical size and bit densities of the chipless tags utilized in examples of the present technology along with various SAR types of technologies, operating frequencies of the RFID reader device may be in the range of 60 GHz up
25 through 240 GHz, by way of example only, although other frequencies may be utilized. In one example, the RFID reader device is configured to operate at 240 GHz with an associated wavelength (λ) of 1.25 millimeters. The RFID reader device may be formed using silicon germanium semiconductor process, such as disclosed in Bredendiek, C. et al., "A 240 GHz single-chip radar transceiver in a SiGe bipolar

technology with on-chip antennas and ultra-wide tuning range,” IEEE Radio Frequency Integrated Circuits Symposium (2013) and “High-Resolution 240-GHZ Radar with SiGe Chip”, Fraunhofer Institute for High Frequency Physics and Radar Techniques FHR (2018), the disclosure of which are hereby incorporated by reference
5 in their entirety. In another example, examples of the present technology may utilize RFID SAR operating frequencies up through 1 THz with the increase in higher resolution printing technologies.

[0036] Those of ordinary skill in the art of short-range FMCW radar will understand the system parameters for designing radars that work effectively from a
10 few centimeters up through hundreds of meters. In examples of the present technology, the transmitter frequency and the receiver frequency are phase locked together, and are simultaneously frequency modulated with a continuous ramp signal, or swept, over a large frequency range. In one example embodiment, the RFID reader device provides a 60 GHz FMCW radar that is swept from 57.4 GHz to 60.9 GHz, or a
15 3.5 GHz sweep bandwidth. In another example, the RFID reader device uses a 60 GHz FMCW radar that is swept from 57 GHz to 71 GHz, or a 14 GHz sweep bandwidth. In yet another example, the RFID reader device uses a 120 GHz FMCW radar that is swept from 110 GHz to 130 GHz, or a 20 GHz sweep bandwidth. And in a further example, the RFID reader device provides a 240 GHz FMCW radar is swept
20 from 220 GHz to 260 GHz, or a 40 GHz sweep bandwidth. As the swept bandwidth is increased, the SAR resolution and signal to noise and signal to clutter ratio is increased.

[0037] Referring now more specifically to FIGS. 2A and 2B, the exemplary fully polarimetric RFID reader device includes antennas, separate transmitter and
25 receiver pairs for vertical polarization and horizontal polarization, a local oscillator, a frequency synthesizer, baseband mixers, low pass filters, and a RFID reader computing device, although the RFID reader device may include other types and/or numbers of other elements or components in other combinations such as additional electronics.

[0038] Referring to FIG. 2A, the antennas used in this example are small aperture, millimeter wave horn type antennas with a 20° radiation beamwidth pattern, although other antenna types and other beamwidths may be used depending upon the specific RFID application. The antennas are coupled to the pairs of transmitters and receivers. More specifically, as shown in FIG. 2A the exemplary RFID reader device includes a horizontal channel transmitter and receiver and a vertical channel transmitter and receiver each coupled to antennas, although other architectures may be employed.

[0039] Referring to FIGS. 3A and 3B, an example of the antenna configuration for the RFID reader device of examples of the present technology is illustrated. Referring more specifically to FIG. 3A, the E-field or polarization sense (arrows) for each antenna is shown. The antennas are arranged with horizontal polarization transmit (H_{TX}) and vertical polarization transmit (V_{TX}) on the top row, and vertical polarization receive (V_{RX}) and horizontal polarization receive (H_{RX}) along the bottom row, although other configurations may be employed. The transmitters and receivers, and their associated antennas are mounted at close spacing to emulate a monostatic radar architecture. Using millimeter wave for the radar operating frequency results in small antenna aperture dimensions, on the order of a few centimeters, which allows close physical spacing.

[0040] Referring again to FIG. 2A, the local oscillator is coupled to the transmitters and receivers to provide an external local oscillator (LO) source radio frequency (RF) signal an inputs to both pairs of transmitters and receivers (horizontal and vertical channels). Those of ordinary skill in the art of radio system design will recognize the double conversion architecture.

[0041] Referring to FIGS. 4A and 4B, examples of the radar transmitter IC and radar receiver IC internal block diagrams are illustrated. In one example, the semiconductor process technology used for the transmitters and receivers in the RFID

reader device is silicon germanium (SiGe), however other semiconductor process technologies may be used in other examples.

[0042] Within the transmitter and receiver integrated circuits, the LO signal frequency is divided by two, which produces the internal intermediate frequency (IF) signal. The LO signal frequency is also frequency multiplied by 3 which produces a final mixer LO signal. Since the IF frequency tracks any change in the LO frequency, this particular superheterodyne approach is known as a sliding-IF design. The transmitter IF signal is applied in-phase, and in-quadrature phase (delayed by 90° or $\pi/2$ radians), to the baseband input mixers, known as the in-phase (I) and quadrature-phase (Q) mixers. The transmitter I and Q input mixers accept external baseband modulation signals that result in the internal IF signal becoming vector modulated. The receiver I and Q output mixers are connected to produce demodulated baseband signals at the I and Q outputs.

[0043] The LO frequency signal is connected to the divide-by-2 circuit that creates the IF frequency, and the LO frequency signal is also connected to the multiply-by-3 circuit which is in turn connected to the final up conversion mixer such that the relationship of the final carrier frequency is shown in equation (3).

$$f_c = 3.5(LO) \quad (1)$$

[0044] Therefore, in one example, when the LO is swept from 16.4 GHz to 17.4 GHz, the resulting FMCW signal at the carrier frequency is swept from 57.4 GHz to 60.9 GHz, although other LO frequencies may be utilized to provide other bandwidth sweep ranges such as described above. The I/Q baseband balanced mixers in the transmitter require I and Q baseband signals in order to produce an IF modulated signal at the outputs.

[0045] The use of pairs of transmitters and receivers for the vertical and horizontal channel requires the ability to distinguish the vertical carrier signal from the

horizontal carrier signal. In this example, the method employed to distinguish the vertical carrier signal from the horizontal carrier signal is provided by a frequency offset, or shift, by controlling the baseband modulating signals generated from the fixed frequency synthesizer, although other methods may be employed.

5 [0046] In this example, referring again to FIG. 2A, the transmitters are also coupled to the frequency synthesizer. The vertical polarization transmitter is driven by I and Q baseband signals in quadrature, meaning the I signal is at zero phase reference (cosine) and the Q signal is driven at 90° or $\pi/2$ radians phase delay (sine) at a fixed frequency of 99.96 MHz from the frequency synthesizer, although other frequencies
10 may be employed. In this example, the horizontal polarization transmitter is driven by I and Q baseband signals also in quadrature at a fixed frequency of 100.00 MHz from the frequency synthesizer, but other frequencies may be used. The vertical polarization and horizontal polarization carrier frequencies are therefore offset by 40 kHz, which provides a method for identifying the receive vertically polarized signals
15 and the receive horizontally polarized baseband signals at the final SAR processing stage, as described in further detail below. Other baseband signal frequencies may be utilized that would result in other offset frequencies.

[0047] Referring now to FIG. 2B, a block diagram of the subcarrier down conversion, data acquisition, and signal processing parts of the RFID reader device
20 performed by the RFID reader computing device is illustrated. In this example, receiver I and Q baseband output signals for both the vertical polarization and horizontal polarization channels, centered at 99.60 MHz and 100.00 MHz respectively, are down converted by baseband mixers to low frequency signals, denoted as subcarrier baseband signals, which are then filtered using low pass filters
25 and are connected to the data acquisition unit. By using a 100.01 MHz fixed frequency LO signal, generated from the fixed frequency synthesizer connected to the baseband mixers, the resulting subcarrier frequency for the vertical polarization receiver signal is centered at 50 kHz ($100.01 \text{ MHz} - 99.96 \text{ MHz} = 50 \text{ kHz}$), while the

resulting subcarrier frequency for the horizontal polarization receiver signal is centered at 10 kHz (100.01 MHz – 100.00 MHz = 10 kHz).

[0048] By utilizing the down conversion to the low frequency subcarrier baseband signals, the frequency content of interest is in the spectral region well below
5 100 kHz, which allows the data acquisition unit to operate at a low sampling rate. Using a low sample rate for the analog to digital conversion in the data acquisition unit allows efficient digital signal conversion at a low cost. In one example, the sample rate of the data acquisition unit is 200 kHz, allowing up to 100 kHz spectral content to be sampled. In order to prevent signal aliasing of any signal energy above 100 kHz,
10 the low pass filters shown in Figure 2B have a roll-off corner of 80 kHz. The data acquisition unit converts the analog subcarrier baseband signals to discrete digital samples that are stored and processed by the SAR signal processing software algorithms that may be implemented in the RFID reader computing device. In one example, the RFID reader computing device is a microcomputer or integrated circuit
15 that may be located on the same chip as the antenna elements for the FMCW radar, but other devices may be used such as a digital signal processor (DSP) or a field programmable logic array (FPGA) by way of example only.

[0049] In another example, the RFID reader computing device includes one or more processor(s), a memory, and/or a communication interface, which are coupled
20 together by a bus or other communication link, although the RFID reader computing device can include other types and/or numbers of elements in other configurations. In one example, the RFID reader computing device is a microcontroller located on the same chip as the millimeter wave radiofrequency device.

[0050] The processor(s) of the RFID reader computing device may execute
25 programmed instructions stored in the memory for the any number of the functions described and illustrated herein. In one example, the processor(s) provides instructions for receiving SAR radar image data from the millimeter wave antennas and processes the radar image data to decode information stored on chipless RFID tags

as described further below. The processor(s) may include one or more CPUs, GPUs, or general purpose processors with one or more processing cores, for example, although other types of processor(s) can also be used.

5 [0051] The memory stores these programmed instructions for one or more aspects of the present technology as described and illustrated herein, although some or all of the programmed instructions could be stored elsewhere. A variety of different types of memory storage devices, such as random access memory (RAM), read only memory (ROM), hard disk, solid state drives, flash memory, or other computer readable medium which is read from and written to by a magnetic, optical, or other
10 reading and writing system that is coupled to the processor(s), can be used for the memory.

[0052] Accordingly, the memory of the RFID reader computing device can store one or more applications or programs that can include computer executable instructions that, when executed by the RFID reader computing device, cause the
15 RFID reader computing device to perform actions described below. The application(s) can be implemented as modules, threads, pipes, streams, or components of other applications. Further, the application(s) can be implemented as operating system extensions, module, plugins, or the like.

[0053] Even further, the application(s) may be operative in a cloud-based
20 computing environment. The application(s) can be executed within or as virtual machine(s) or virtual server(s) that may be managed in a cloud-based computing environment. Also, the application(s) may be running in one or more virtual machines (VMs) executing on the image acquisition computing device. The communication interface operatively couples and communicates between the RFID reader computing
25 device and the millimeter wave radiofrequency antennas.

[0054] In another example, the RFID reader computing device is a highly integrated microcontroller device with a variety of on-board hardware functions, such as analog to digital converters, digital to analog converters, serial buses, general purpose I/O pins, RAM, and ROM. The microcontroller may be located on the same

chip as the millimeter wave radiofrequency antenna devices of the RFID reader device, by way of example.

[0055] Although the exemplary RFID reader computing device is described and illustrated herein, other types and/or numbers of systems, devices, components, and/or elements in other topologies can be used. It is to be understood that the systems of the examples described herein are for exemplary purposes, as many variations of the specific hardware and software used to implement the examples are possible, as will be appreciated by those skilled in the relevant art(s).

[0056] In addition, two or more computing systems or devices can be substituted for the RFID control computing device. Accordingly, principles and advantages of distributed processing, such as redundancy and replication also can be implemented, as desired, to increase the robustness and performance of the devices and systems of the examples. The examples may also be implemented on computer system(s) that extend across any suitable network using any suitable interface mechanisms and traffic technologies, including by way of example only teletraffic in any suitable form (*e.g.*, voice and modem), wireless traffic networks, cellular traffic networks, Packet Data Networks (PDNs), the Internet, intranets, and combinations thereof.

[0057] The examples may also be embodied as one or more non-transitory computer readable media having instructions stored thereon for one or more aspects of the present technology as described and illustrated by way of the examples herein. The instructions in some examples include executable code that, when executed by one or more processors, cause the processors to carry out steps necessary to implement the methods of the examples of this technology that are described and illustrated herein.

[0058] Referring now more specifically to FIGS. 1 and 5-9, an example of the system of the present technology includes a plurality of chipless RFID tags that may be employed with the RFID reader device described above. In this example, the RFID tags include a plurality of microstrip patch antenna elements that are formed on a

substrate. As described in further detail below, the microstrip patch antenna elements are oriented and have dimensions to provide polarization and phase information representative of the information encoded on the RFID tag, which can be read-out by the RFID reader device. The microstrip patch antenna elements re-radiate
5 radiofrequency signals received from the RFID reader device back to the RFID reader device to form a radar image.

[0059] Construction of the chipless tag in examples of the present technology uses the microstrip patch antenna as the fundamental encoding element. Referring to FIG. 5 an exemplary microstrip patch antenna element in relation to the substrate used
10 as the RFID label is shown. Those of ordinary skill in the art of microstrip patch antenna design will be familiar with the technique for design and construction. The equations below determine the physical dimensions of width, W , and length, L , of the microstrip patch antenna element as a function of the dielectric constant of the substrate material (ϵ_R), the thickness of the substrate (h), and the operating frequency
15 (f_0).

$$\begin{aligned} \text{Width} &= \frac{c}{2f_0\sqrt{\frac{\epsilon_R+1}{2}}}; \quad \epsilon_{eff} = \frac{\epsilon_R+1}{2} + \frac{\epsilon_R-1}{2} \left[\frac{1}{\sqrt{1+12\left(\frac{h}{W}\right)}} \right] \\ \text{Length} &= \frac{c}{2f_0\sqrt{\epsilon_{eff}}} - 0.824h \left(\frac{(\epsilon_{eff}+0.3)\left(\frac{W}{h}+0.264\right)}{(\epsilon_{eff}-0.258)\left(\frac{W}{h}+0.8\right)} \right) \end{aligned} \quad (2)$$

The substrate material or label stock also has a conductor on the opposite side which acts as a ground plane. By using the microstrip patch antenna with ground plane allows the tag to be placed on any item even if the item is electrically conductive, such
20 as metal containers, cans, and liquid containers without affecting the antenna element properties.

[0060] The microstrip patch antenna elements of examples of the present technology may be printed using any conductive material. As set forth below,

examples of the system of the present technology rely on antenna reradiation, which does not require high electrical conductivity printing material to create the tag antenna elements. Prior art devices that use spectral signature or resonance detection, limits the number of discernable spectral signature states on resonate frequency

5 discrimination, which in turn depends on the circuit resonance quality (Q) factor. The Q factor is directly dependent on the electrical conductivity and is mainly determined by the physical relation of the ratio of inductive reactance (X_L) to the resistance (R), as shown in equation (3).

$$10 \quad Q = \frac{X_L}{R} \quad (3)$$

[0061] The specific electrical resistance of a material is specified by its resistivity, and is measured in ohm-m (ρ), but often when specifying a material's ability to conduct electricity, the inverse of resistivity, or conductivity (σ) is used. The unit of conductivity is measured in siemens per meter (S/m). It is important to note that in prior art devices that detect spectral signature states, the dependence on materials with very high conductivity, such as silver, is needed to achieve maximum spectral signature or resonant frequency discrimination.

[0062] In examples of the present technology, which use antenna reradiation in a SAR RFID system, a useful characteristic measurement for a target, or tag antenna element, is the radar cross section (RCS). RCS is a measure of the target's ability to reradiate and reflect the radar energy that illuminates the antenna element area. Those of ordinary skill in the art of radar engineering use RCS as a deterministic method to compare various radar targets in the ability to efficiently reradiate and reflect the impinging radar electromagnetic energy.

[0063] Simulation of the RCS of a conductive sheet as a function of sheet electrical conductivity illustrates the relative independence of the RCS with respect to the sheet electrical conductivity. Referring to FIG. 11, the results of simulating a 10 mm x 10 mm x 1 μ m conductive sheet at 60 GHz are shown, illustrating that even with

material conductivities as poor as those from zinc, nickel, lead or even iron do not change the RCS values.

[0064] The graph in FIG. 12, and the associated table of material conductivities shows that inks for printed RFID antenna structures can use a wide variety of low-cost conductive materials without impact to the RCS value, and therefore without impact to the reradiation signal strength in the SAR radar system. Arbitrary conductivities were chosen for “ink” values from 2.2×10^7 down to 5.0. Any value for the conductivity greater than 1.0×10^6 results in the same RCS value. Thus, various conductive materials may be used to print the microstrip patch antennas of the present technology, which significantly reduces the costs to produce the chipless tags employed in the system of the present technology.

[0065] Examples of the present technology uses increased operating frequency for the RFID reader device, as described above, which reduces the wavelength of the system. This allows for manufacturing chipless tags with increased bit densities. As set forth above, recent technological advances in silicon technology has enabled the ability to produce operating radars at frequencies as high as 240 GHz, with the associated wavelength (λ) reduced to 1.25 mm, such as disclosed in Bredendiek, C. et al., “A 240 GHz single-chip radar transceiver in a SiGe bipolar technology with on-chip antennas and ultra-wide tuning range,” IEEE Radio Frequency Integrated Circuits Symposium (2013) and “High-Resolution 240 GHz Radar with SiGe Chip”, Fraunhofer Institute for High Frequency Physics and Radar Techniques FHR (2018), the disclosure of which is hereby incorporated by reference in its entirety.

[0066] Using microstrip patch millimeter wave antenna elements printed on the RFID tag, with element dimensions on the order of $\frac{1}{2} \lambda$, a greater quantity of tag elements can be achieved in a given area compared with lower frequency resonant lumped-element circuits or meandered strip lines. Further, by using microstrip patch antenna elements rather than circuit resonators based on either lumped-element or strip

line geometries, control of polarization and phase parameters is used to significantly increase the number of encoded bits per element.

[0067] For practical size and bit densities to be considered using various SAR types of technologies, frequencies are described in examples of the present technology, but not limited to, the range of 60 GHz up through 240 GHz. Over this millimeter wave frequency range, practical SAR RFID chipless tags tradeoff bit density versus state of the art tag element printing resolution. As conductive or metallic printing technology moves forward with higher resolution capabilities, the higher millimeter wave frequencies, and corresponding smaller wavelengths, can be used to create higher bit densities.

[0068] Referring now more specifically to FIG. 6A, as an example, an RFID system operating at a millimeter wave frequency of 60 GHz, with $\lambda = 5.0$ mm, a practical $\frac{1}{2} \lambda$ microstrip patch antenna printed on a dielectric or label substrate with a thickness of 0.25 mm material has a printed dimension of 1.8 mm x 1.3 mm. The substrate or label material has an associated electrically conductive ground plane layer on the opposing side to the antenna elements, and the dielectric constant is 3.0. The microstrip patch antenna element impedance and size is controlled by the dielectric or label material thickness and dielectric constant.

[0069] Maintaining low inter-element coupling allows the ability to image and resolve the phase and polarization states of each element independently within an array of multiple elements. At an element size of 1.8 mm x 1.3 mm, with optimal low intercoupling antenna element spacing of 1λ , or 5.0 mm, 25 elements can be printed within an approximate 1 square inch (6.8 square cm) area. In this example at 60 GHz, the total bit density is 25 elements/square inch. With a 64 state encoding scheme for polarization and phase described below producing 6 bits/element of encoding density, 25 elements/square inch x 6 bits/element provides approximately 150 bits/square inch (approximately 22 bits/square centimeter) of encoding bit density in this example.

[0070] Referring to Figure 6A, an array of microstrip patch antenna elements on a representative RFID tag operating in an RFID system at 60 GHz with dimensions indicated is illustrated. The specific microstrip patch antennas shown in the drawing are for reference only so as to indicate relative position and spacing between the microstrip patch antennas. A typical printed tag will have different antenna element rotational orientations for encoding polarization states and different antenna phase tails for encoding phase states as described below.

[0071] Referring now more specifically to FIG. 6B, in another example, an RFID system operating at a frequency of 120 GHz, with $\lambda = 2.5$ mm, a practical $\frac{1}{2} \lambda$ patch antenna printed on a dielectric or label substrate with a thickness of 0.25 mm material has a printed dimension of approximately 0.9 mm x 0.6 mm. With an element spacing of 1λ , or 2.5 mm, 100 elements can be printed within approximately 1 square inch area. With the 64 state encoding scheme for polarization and phase described below producing 6 bits/element of encoding density, 100 elements/square inch x 6 bits/element provides approximately 600 bits/square inch (approximately 89 bits/square centimeter) of encoding bit density.

[0072] In Figure 6B, an array of microstrip patch antenna elements on a representative tag substrate is shown for an RFID system operating at 120 GHz. Note that by reducing the associated wavelength by $\frac{1}{2}$ relative to the 60 GHz system, that approximately four times the number of elements can be printed in an equivalent tag area.

[0073] Referring now to more specifically to FIG. 6C, in yet another example, an RFID system operating at a frequency of 240 GHz, with $\lambda = 1.25$ mm, a practical $\frac{1}{2} \lambda$ antenna printed on a dielectric or label substrate with a thickness of 0.25 mm material has a printed dimension of 0.4 mm x 0.2 mm. With an element spacing of 1λ , or 1.25 mm, 400 elements can be printed within approximately 1 square inch area. With the 64 state encoding scheme for polarization and phase described below producing 6 bits/element of encoding density, 400 elements/square inch x 6

bits/element provides approximately 2400 bits/square inch (approximately 355 bits/square centimeter) of total encoding bit density.

5 [0074] In Figure 6C, an array of microstrip patch antenna elements on a representative tag is shown for an RFID system operating at 240 GHz. The current system constraint on higher frequency, and shorter associated wavelength, RFID systems is limited by the printing resolution for placing the conductive materials onto a tag substrate. As printing technologies advance that can produce higher resolution tag elements, higher frequency chipless RFID systems can be developed and utilized with this technology. Examples of this technology may utilize RFID SAR operating 10 frequencies up through 1 THz.

[0075] As can be seen from this relationship between tag encoding bit density and operating frequency, as the operating frequency is doubled, the total bit density is quadrupled. Achieving higher bit densities requires printing the greatest allowable number of microstrip patch antenna elements in a given area on the chipless RFID tag. 15 As the distance between microstrip patch antenna elements is decreased in order to increase the number of elements per tag area, there can be inter-element coupling which can reduce the detection of the individual element polarization and phase states for the microstrip patch antenna elements. The main contributing mechanism to inter-element coupling at millimeter waves is surface wave propagation along the surface of the dielectric substrate. In examples of the present technology, the inter-element 20 coupling is reduced by spacing the microstrip patch antenna elements at least 1 wavelength (1λ) apart on the chipless RFID tag, but other methods of reducing the inter-element coupling may be employed. Since the wavelength dimension at millimeter waves is relatively small in comparison with typical chipless RFID tag sizes, the number of elements that can be printed achieves high bit densities. 25

[0076] Referring again to FIG. 5, the microstrip patch antenna element has an inherent polarization, or E-field orientation. The polarization state of the patch is one of the variables used to encode information. By printing the microstrip patch with

different rotational orientations, different polarization states will be exhibited relative to the reader orientation. In examples of the present technology, up to 8 discrete rotational orientations representing up to 8 polarization states are utilized, but in other examples more polarization states are possible.

5 [0077] Referring to FIG. 7, examples of the microstrip patch antenna elements with different rotational orientations are illustrated. The arrows represent the E-field direction that defines the antenna element polarization. In the present invention, the fully polarimetric SAR RFID device, as described above, allows detection of the polarization state of the target microstrip patch antenna element.

10 [0078] Referring now to FIG. 8, the other parameter used for encoding information into the antenna element is the phase state of the micropatch antenna. In examples of the present technology, control of the microstrip patch antenna phase state is achieved through the use of small transmission line “tails” added to the patch as shown in FIG. 8, but other methods of phase control are contemplated. By way of
15 example only, other geometries may be utilized to provide phase control. In this example, the length of the added tail sets the phase delay response of the patch antenna element. Tails with shorter lengths will have shorter delay response times or lower phase delay, while tails with longer lengths will have longer phase delay times. In examples of the present technology, up to 8 discrete tail lengths represent up to 8
20 discrete phase states but in other examples more phase states are possible.

[0079] Referring now of FIG. 9, exemplary microstrip antenna elements having both a polarization state and a phase state as described above are illustrated. By combining the polarization states and phase states for the microstrip antenna elements on the chipless RFID tag, both parameters can be used for encoding data. In
25 examples of the present technology, up to 8 polarization states and up to 8 phase states combinatorically provide 64 (8 x 8) unique states per microstrip antenna element, but more polarization and phase states are contemplated. The number of binary bits represented by 64 states is found by $\log_2(64) = 6$ bits per element.

[0080] An exemplary operation of the RFID system of examples of the present technology will now be described with reference to FIGS. 1-10. The SAR image processing described below with polarization and phase discrimination is used for any of the above types of SAR radar architectures.

5 [0081] First, the RFID reader device transmits electromagnetic radiation to a scan area. The electromagnetic radiation is provided at the sweep frequency determined by the local oscillator. In one example, the RFID reader device provides a 60 GHz FMCW radar that is swept from 57.4 GHz to 60.9 GHz, or a 3.5 GHz sweep bandwidth. In another example, the RFID reader device uses a 60 GHz FMCW radar
10 that is swept from 57 GHz to 71 GHz, or a 14 GHz sweep bandwidth. In yet another example, the RFID reader device uses a 120 GHz FMCW radar that is swept from 110 GHz to 130 GHz, or a 20 GHz sweep bandwidth. And in a further example, the RFID reader device provides a 240 GHz FMCW radar is swept from 220 GHz to 260 GHz, or a 40 GHz sweep bandwidth, although other frequencies may be employed. The
15 electromagnetic radiation is polarized through the horizontal and vertical transmitters such that the system is fully polarimetric.

[0082] In order to generate the synthetic aperture, either the chipless RFID tag or the RFID reader device are in motion, although other methods may be employed. In a wide sweep bandwidth ISAR mode, the axis of rotation or in a path of a linear
20 movement of the tag, such as in a conveyor system, will be at an angle of inclination (incidence angle) which will yield high range resolution that will enable two dimensional tag element imaging capability. The inclined angles may used in wide sweep bandwidth SAR modes, such as a drone carrying the radar platform for larger area RFID logistics applications.

25 [0083] Next, the electromagnetic radiation is received at the RFID tags in the scanned area, causing the micropatch antenna element structures of the RFID tags to resonate at the desired frequency and re-radiate the electromagnetic signals back toward the RFID reader device. In an FMCW radar system with relatively short

distances from the radar (RFID reader) to the target (chipless tag), the typical difference between the transmitter and receiver frequency, known as the FMCW beat frequency, is low enough to be sampled easily by a low sample rate analog to digital converter. This is the main advantage of using FMCW for short range applications such as SAR RFID systems where distances range from a few cm up to tens of meters. In an example, the FMCW parameters for sweep bandwidth (B_{SW}) and sweep time (T_S), also known as the chirp time, are shown in FIG. 13.

[0084] Those of ordinary skill in the art of FCMW radar will be familiar with the equations that define FCMW parameters. The round-trip delay time (T_D), which determines the difference between the receive frequency and the transmit frequency is found by equation (4), where c is the speed of light, and R is the range or distance between the radar and the target, as shown in Figure 15.

$$T_D = \frac{2R}{c} \quad (4)$$

[0085] The difference between the FMCW transmit frequency and receive frequency is also known as the beat frequency (f_B). The beat frequency is a function of the sweep bandwidth (B_{SW}), the time delay (T_D) and the chirp time (T_S) as shown in equation (5).

$$f_B = \frac{B_{SW} T_D}{T_S} \quad (5)$$

[0086] In an example, SAR RFID system, with a range, R , of 1m from the radar to the tag, the round-trip time delay comes out to 6.67 ns. In the example SAR RFID system with the FMCW sweep parameters as shown in FIG. 13, the beat frequency, f_b is equal to 2.34 kHz. In an example, the FMCW transmitter quadrature baseband signaling frequency for the vertical polarization channel is 99.96 MHz, and the quadrature baseband signaling frequency for the horizontal polarization channel is

100.00 MHz, and the subcarrier baseband conversion LO frequency is 100.01 MHz. The down converted subcarrier baseband frequency for the vertical polarization channel is 50 kHz, and the down converted subcarrier baseband frequency for the horizontal polarization channel is 10 kHz. The receive beat frequency (f_B) is added to the subcarrier frequency values and in the example system, with a 1 meter tag distance, the final subcarrier frequency for the vertical polarization channel is 52.34 kHz, and for the horizontal polarization channel is 12.34 kHz, although other frequencies may be employed.

[0087] The received re-radiated electromagnetic radiation from the chipless tag is received by the receiver and converted to subcarrier signals in the downconversion process described above, although other methods may be employed. Next, the data acquisition unit converts the received subcarrier signals from the vertical polarization receiver signal and the horizontal polarization receiver signal into data. In one example, the data acquisition unit (DAQ) samples and converts the voltage levels into digital values at a rate of 200 kilo-samples per sec, or 200 kS/s. The sequence of stored data samples is known in the art as the phase history. A small segment of a stored sample file illustrating a phase history is shown in Figure 14. The first column shows the sample sequence number, and remaining columns show the digital values of the voltages taken at each sample instance for the vertical polarization I-channel, vertical polarization Q-channel, horizontal polarization I-channel and the horizontal polarization Q-channel.

[0088] The standard nomenclature used in SAR polarimetric radar is to specify the transmit polarization and receive polarization by a two letter acronym, using V for vertical polarization and H for horizontal polarization. In referring to the aspect of a polarimetric radar system that transmits the vertical polarization signal and receives the vertical polarization signal, the designation is VV. For the aspect of the polarimetric radar that transmits the vertical polarization signal and receives the horizontal polarization signal, the designation is VH. The four aspect signal

descriptions are VV, HH, HV and VH, which account for all combinations of transmit and receive polarization signals.

[0089] Next, the data from the data acquisition unit is stored, processed and displayed for interpretation by the RFID reader computing device. In one example, visual display of the decoded SAR images is used to demonstrate tag element decoding, although other methods of data representation, communication, and storage may be used, such as RFID data base analysis for inventory control, and logistics and cloud storage for archiving by way of example only.

[0090] Next, SAR signal processing algorithms use the different combinations of signal polarizations to detect and discriminate the polarization signatures and the phase signatures across the spatial domain of the target or tag. An exemplary subcarrier spectrum for both polarizations is shown in FIG. 15. The ISAR (in the case of a moving chipless RFID tag) signal processing is implemented through software algorithms that process the stored data samples acquired through the data acquisition unit. In an example, the receiver I and Q output subcarrier signal voltage levels for both the vertical and horizontal polarization channels range from a few millivolts up to approximately ½ volt peak to peak. The frequency span of the subcarrier voltage signals range up through 80 kHz, depending upon the distance to the tag.

[0091] Once the data samples are stored, the ISAR processing begins. The high-level flowchart shown in Figure 10 describes the full ISAR processing algorithms. In one example, the polarization decoding and phase decoding may be represented as images. The polarization and phase decoding may be stored and sent to various RFID back-end system data bases for application specific uses. The data obtained from the subcarrier signals from the data acquisition unit is loaded by the RFID reader computing device. The RFID reader computing device extracts the data and separates the data based on the transmit and receive polarizations in the four categories (VV, VH, HV, HH). Next, the RFID reader applies a calibration. In this example, the RFID reader computing device then generates images based on the four

different categories of transmit and receive polarizations. The image data may then be used to extract polarization and phase data for individual micropatch antenna element structures on the chipless tag. Images can be generated to represent the polarization and phase, although other methods of identifying polarization and phase may be utilized. The polarization data and phase data may then be decoded to extract the data stored on the tag.

Example

[0092] A 60 GHz radar transmitter and 60 GHz radar receiver were built from silicon germanium (SiGe) application specific integrated circuit (IC) technology both architected as double conversion superheterodyne devices.

[0093] A single row of tag elements with phase and polarization states was evaluated. The radar (reader) platform was held stationary, while the tag was moved in order to create the synthetic aperture. In this example, the tag was rotated using a rotary stage motor as shown in FIG. 16. The tag was moved in a circular arc with its axis perpendicular to the radar.

[0094] Over a sampling period of 20 seconds, approximately 4 million samples (4 MS) were stored and processed. A sampling period of 20 seconds was used to be compatible with the DAQ sampling rate and the rate of storage in the computer system. In examples of this technology, high speed sampling, storage and processing will be implemented to provide near real time RFID tag element decoding.

[0095] The obtained data was processed based on the inverse SAR, or ISAR architecture. The validation of polarization detection was through rendering of different colors on a computer display to extract the polarization data. FIG. 17 shows the polarization renderings for horizontal (0°) polarized tag elements in the color red, a 45° polarized tag element in green, and a vertical (90°) polarized tag element in blue. The choice of the colors for representing polarization angle was arbitrary and was used to provide visual validation of the decoded polarization states.

[0096] In FIG. 18, validation of phase detection was through rendering of different colors on a computer display to extract the phase data. Phase renderings for 0° phase delay in red, 45° phase delay in blue, 90° phase delay in blue-green, and 135° phase delay in white. The choice of the colors for representing phase delay time was
5 arbitrary and was used to provide visual validation of the decoded phase states.

[0097] Having thus described the basic concept of the invention, it will be rather apparent to those of ordinary skill in the art that the foregoing detailed disclosure is intended to be presented by way of example only, and is not limiting. Various alterations, improvements, and modifications will occur and are intended to
10 those skilled in the art, though not expressly stated herein. These alterations, improvements, and modifications are intended to be suggested hereby, and are within the spirit and scope of the invention. Additionally, the recited order of processing elements or sequences, or the use of numbers, letters, or other designations therefore, is not intended to limit the claimed processes to any order
15 except as may be specified in the claims. Accordingly, the invention is limited only by the following claims and equivalents thereto.

CLAIMS

What is claimed is:

1. A method comprising:
 - transmitting, by a radiofrequency identification (RFID reader device), a
5 first millimeter wave radiofrequency beam at a first polarization and second
millimeter wave radiofrequency beam at a second polarization perpendicular to the
first polarization to a chipless RFID tag having a plurality of microstructure elements
located thereon, each of the microstructure elements having a polarization state and a
phase state, wherein the first millimeter wave radiofrequency and the second
10 millimeter wave radiofrequency beams are offset in frequency;
 - receiving, by the RFID reader device, re-radiated millimeter wave
radiofrequency beams from the chipless RFID tag;
 - generating, by the RFID reader device, a radar image based on the re-
radiated millimeter wave radiofrequency beams; and
 - 15 determining, by the RFID reader device, the phase state and the
polarization state of each of the plurality of microstructure elements located on the
chipless RFID tag based on the generated radar image.
2. A RFID reader device comprising:
 - 20 a first millimeter wave radiofrequency transmitter configured to
transmit electromagnetic radiation at a first polarization and a first frequency to a
chipless RFID tag having a plurality of microstructure elements located thereon, each
of the microstructure elements having a polarization state and a phase state;
 - a second millimeter wave radiofrequency transmitter configured to
25 transmit electromagnetic radiation at a second polarization perpendicular to the first
polarization and at a second frequency to the chipless RFID tag;
 - a first millimeter wave radiofrequency receiver configured to receive
re-radiated electromagnetic radiation from the chipless RFID tag at the first
polarization and a second millimeter wave radiofrequency receiver configured to

receive re-radiated electromagnetic radiation from the chipless RFID tag at the second polarization; and

an RFID reader computing device coupled to the first and second radiofrequency receivers, the RFID control computing device comprising a memory coupled to a processor which is configured to be capable of executing programmed instructions comprising and stored in the memory to:

generate a radar image based on the re-radiated millimeter wave radiofrequency beams from the first and second radiofrequency receivers; and
determine the phase state and the polarization state of each of the plurality of microstructure elements located on the chipless RFID tag based on the generated radar image.

3. An RFID system comprising:

at least one chipless RFID tag having a plurality of microstructure elements located thereon, each of the microstructure elements having a polarization state and a phase state; and

an RFID reader device comprising:

a first millimeter wave radiofrequency transmitter configured to transmit electromagnetic radiation at a first polarization and a first frequency to a chipless RFID tag having a plurality of microstructure elements located thereon, each of the microstructure elements having a polarization state and a phase state;

a second millimeter wave radiofrequency transmitter configured to transmit electromagnetic radiation at a second polarization perpendicular to the first polarization to the chipless RFID tag;

a first millimeter wave radiofrequency receiver configured to receive re-radiated electromagnetic radiation from the chipless RFID tag at the first polarization and a second millimeter wave radiofrequency receiver configured to receive re-radiated electromagnetic radiation from the chipless RFID tag at the second polarization; and

an RFID reader computing device coupled to the first and second radiofrequency receivers, the RFID control computing device comprising a memory coupled to a processor which is configured to be capable of executing programmed instructions comprising and stored in the memory to:

- 5 generate a radar image based on the re-radiated millimeter wave radiofrequency beams from the first and second radiofrequency receivers; and
-
- 10 determine the phase state and the polarization state of each of the plurality of microstructure elements located on the chipless RFID tag based on the generated radar image.

4. A chipless RFID tag comprising:

a substrate;

- 15 a plurality of millimeter wave antenna elements printed on the substrate, each of the plurality of millimeter wave antenna elements having a phase state and a polarization state, wherein each millimeter wave antenna element printed on the substrate is located at least one wavelength apart from each other millimeter wave antenna element printed on the substrate.

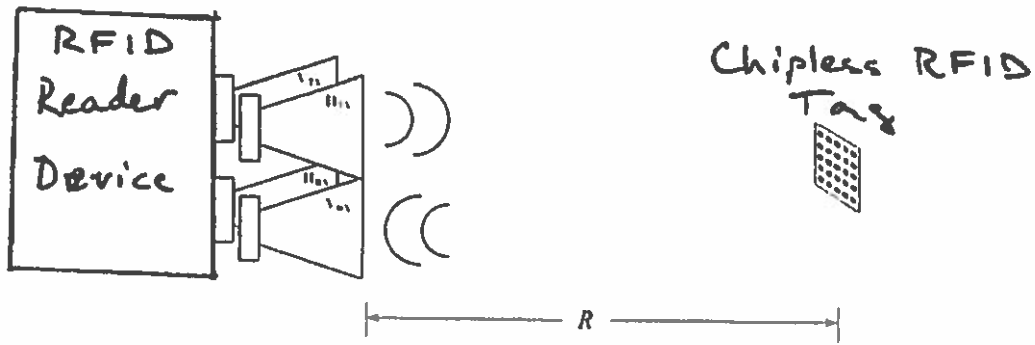


FIG. 1

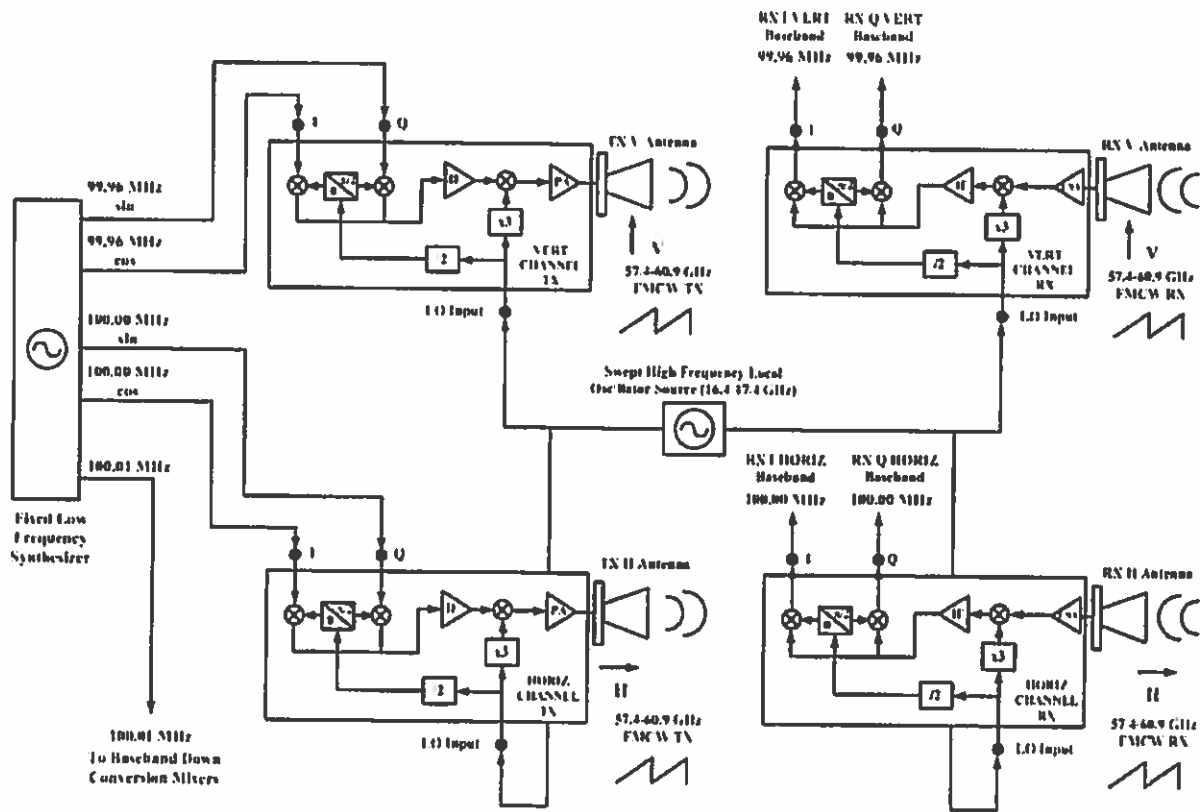


FIG. 2A

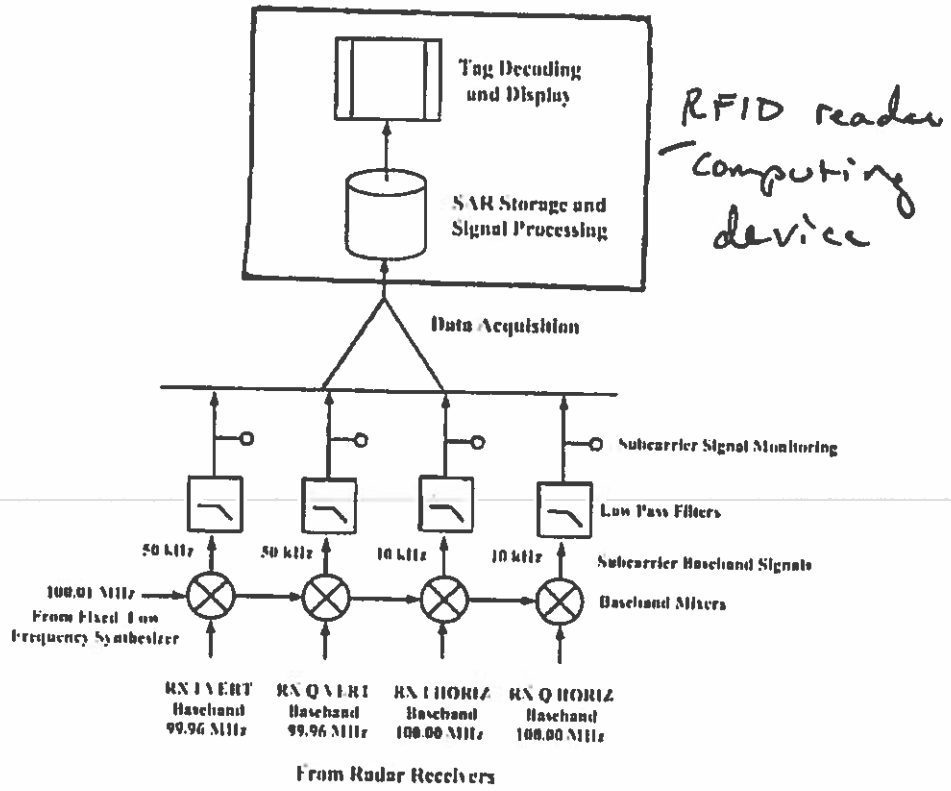


FIG. 2B

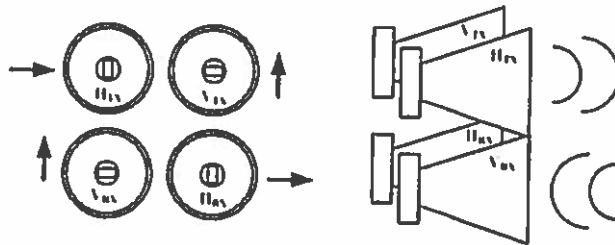


FIG. 3A

FIG. 3B

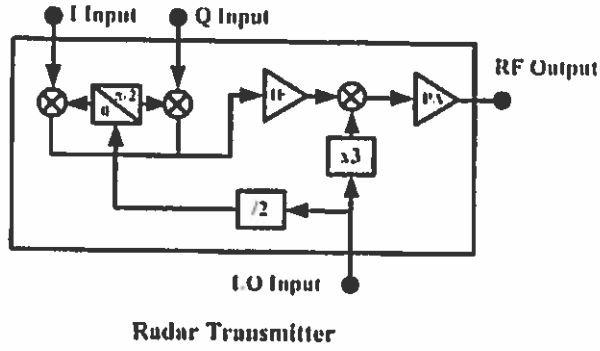


FIG. 4A

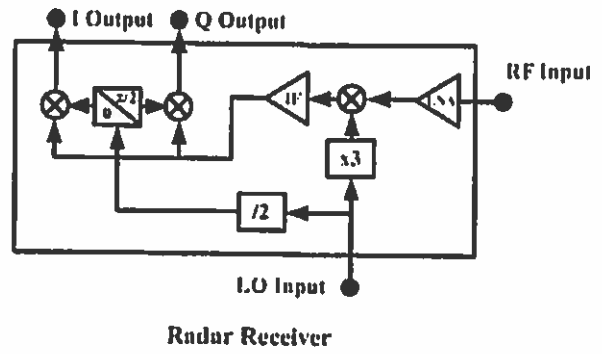


FIG. 4B

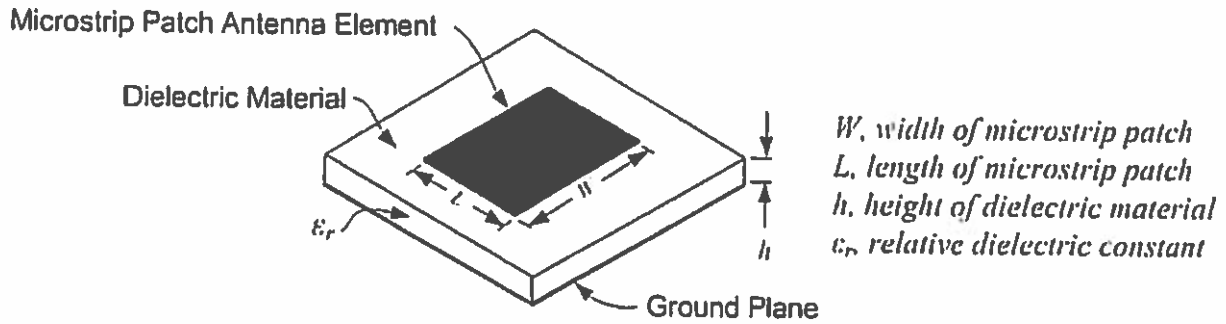


FIG. 5

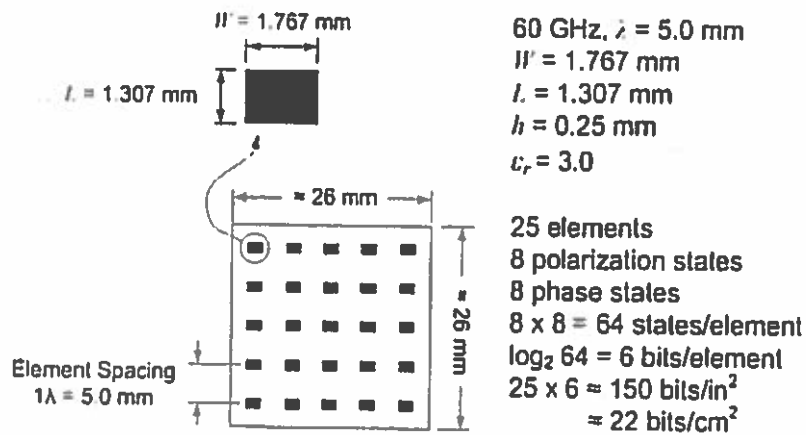


FIG. 6A

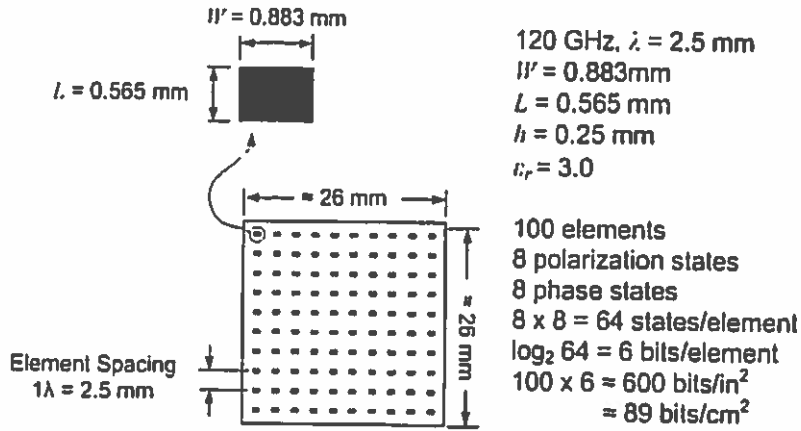


FIG. 6B

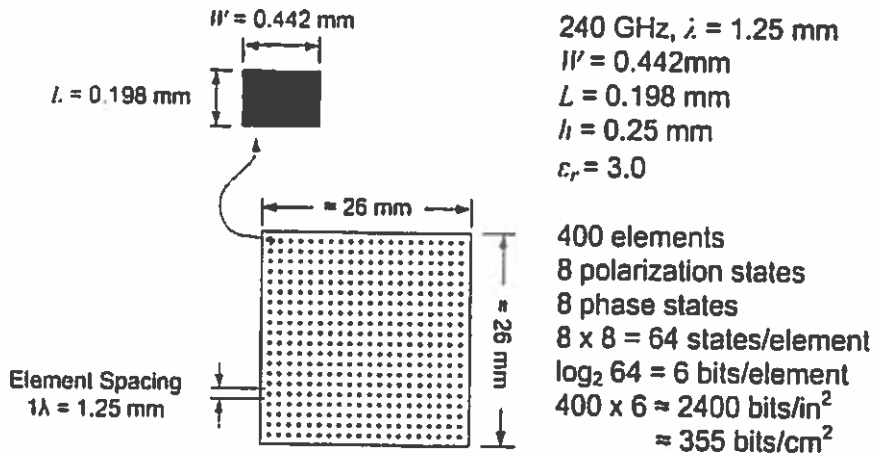


FIG. 6C

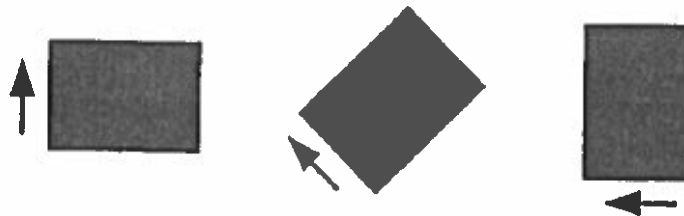


FIG. 7



FIG. 8



FIG. 9

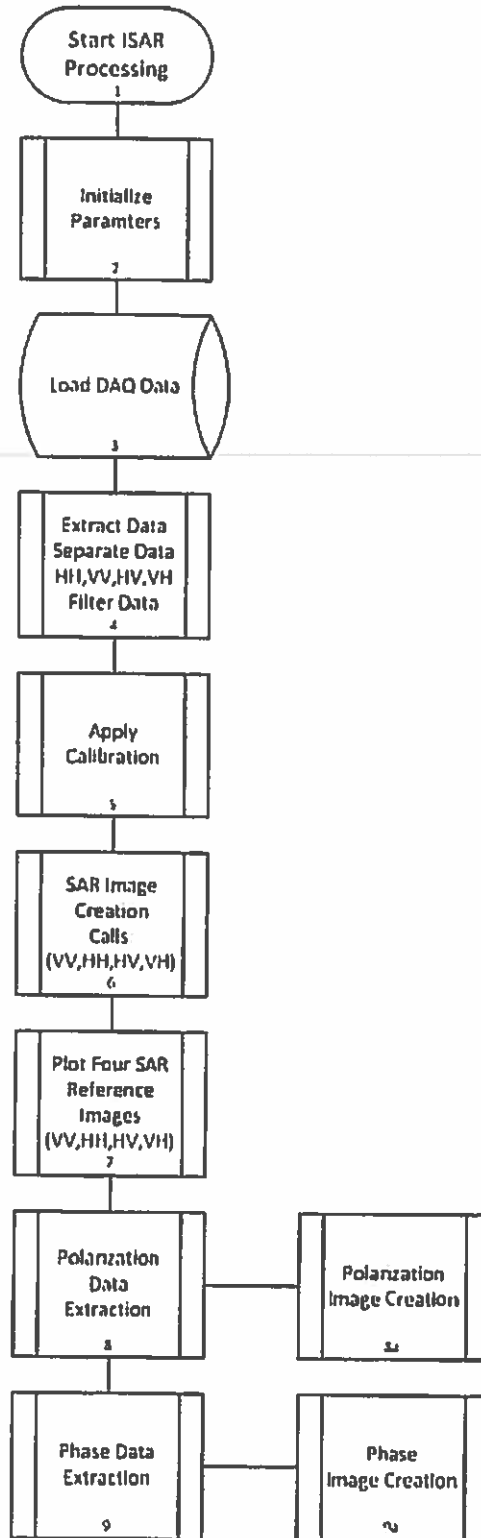
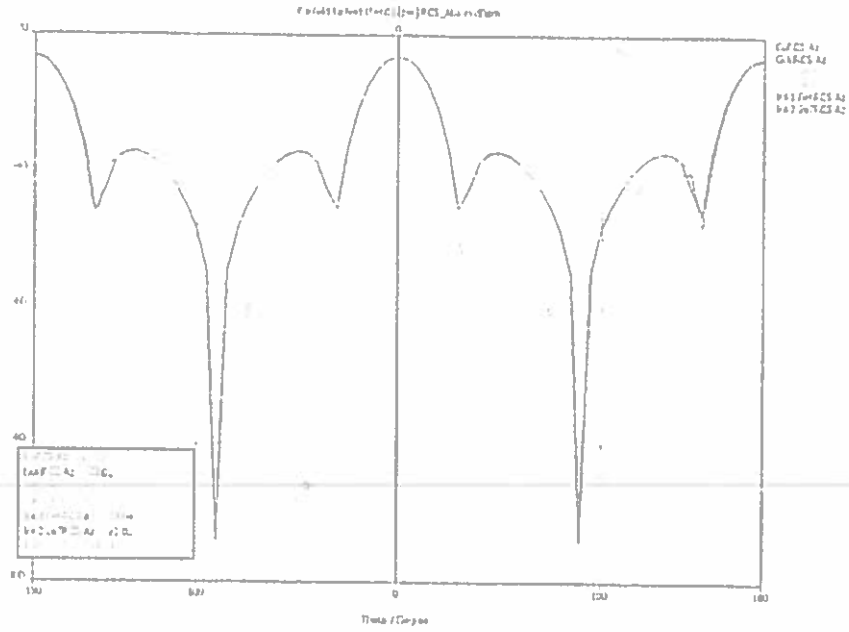


FIG. 10



| Material | Conductivity σ S/m | Resistivity ρ Ohm | RCS σ^m dBsm |
|----------|---------------------------------|------------------------------|---------------------------|
| Copper | 5.80E+07 | 1.72E-08 | -23.02 |
| Gold | 4.09E+07 | 2.44E-08 | -23.02 |
| Ink1 | 2.20E+07 | 4.55E-08 | -23.02 |
| Ink2 | 1.00E+06 | 1.00E-06 | -23.04 |
| Ink3 | 1.00E+02 | 1.00E-02 | -25.96 |
| Ink4 | 1.00E+01 | 1.00E-01 | -31.20 |
| Ink5 | 5.00E+00 | 2.00E-01 | -34.24 |

FIG. 11

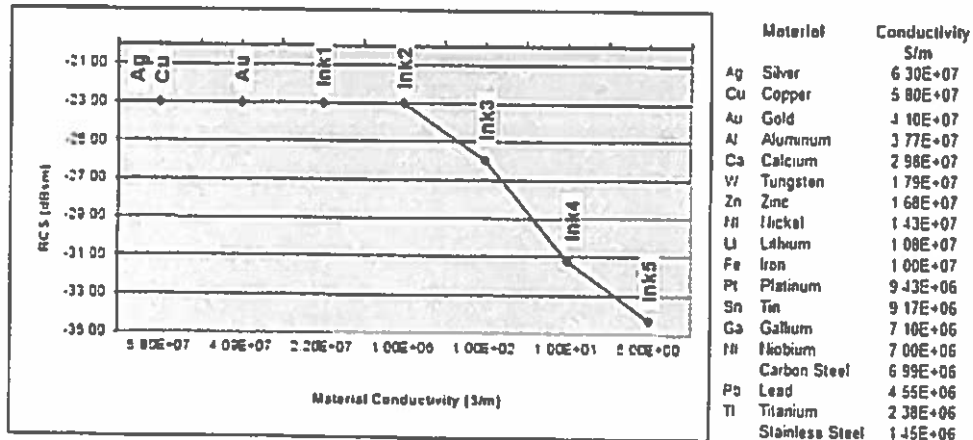


FIG. 12

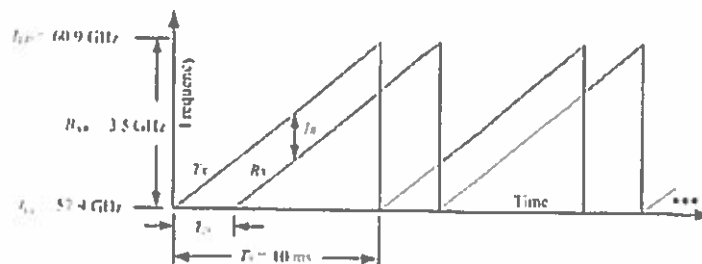


FIG. 13

| SAMPLE (#) | VERT I (V) | VERT Q (V) | HORIZ I (V) | HORIZ Q (V) |
|------------|------------|------------|-------------|-------------|
| 205398 | 0.166508 | 0.233518 | 0.07891 | -0.12899 |
| 205399 | 0.224322 | 0.025361 | 0.001715 | 0.321131 |
| 205400 | 0.132991 | -0.01761 | -0.33589 | 0.006494 |
| 205401 | 0.148929 | 0.011999 | -0.14986 | -0.52261 |
| 205402 | 0.224947 | -0.10771 | 0.203375 | -0.17376 |

FIG. 14

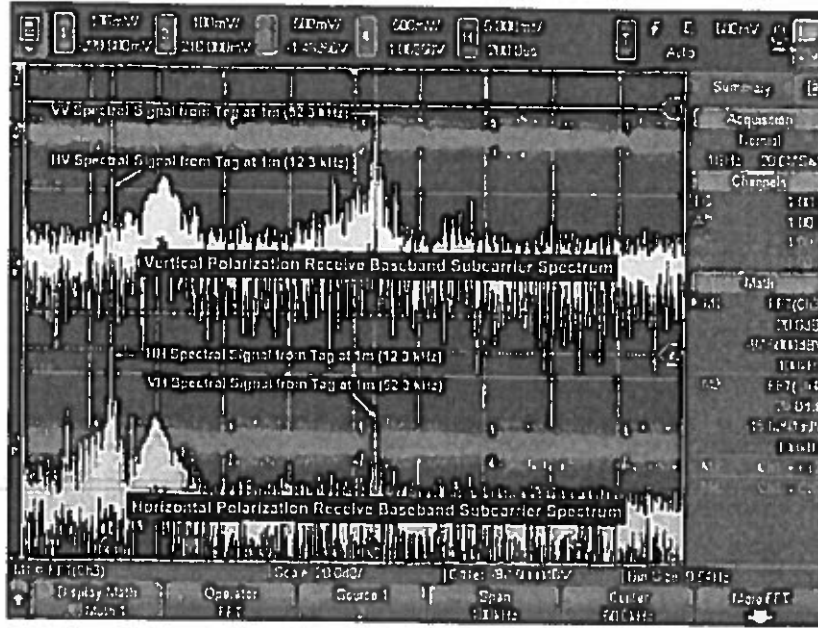


FIG. 15

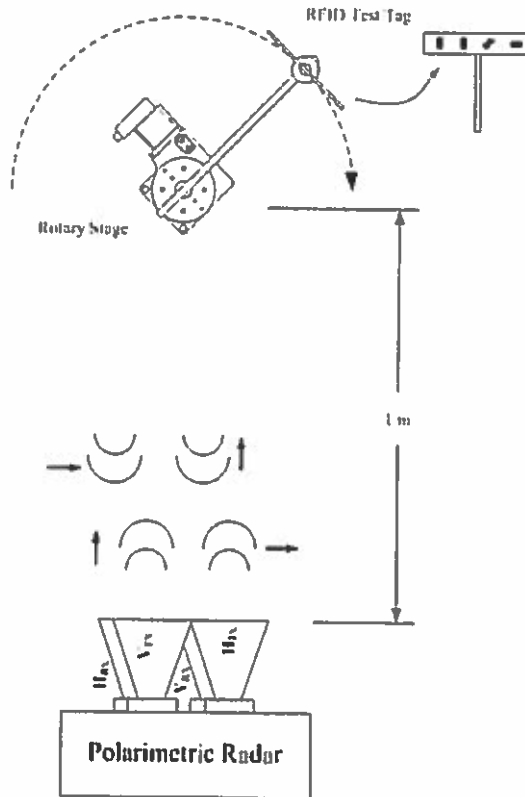


FIG. 16

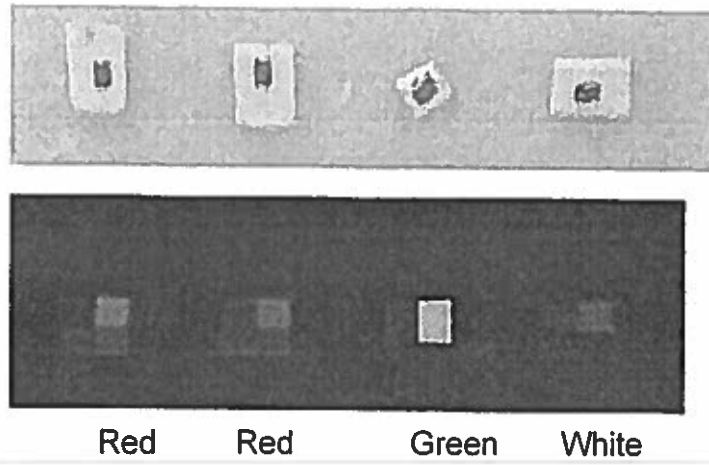
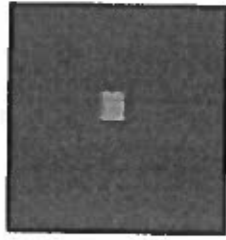
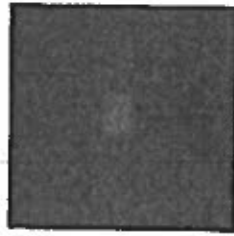


FIG. 17

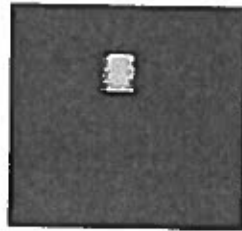
Red



Blue



Blue-Green



White



FIG. 18